Structure and Dynamics of β-Cyclodextrin in Aqueous Solution at the Density-Functional Tight Binding Level†

Thomas Heine,‡ Hélio F. Dos Santos,§ Serguei Patchkovskii,# and Hélio A. Duarte*,⊥

Physikalische Chemie, TU Dresden, D-01062 Dresden, Germany, Núcleo de Estudos em Química Computacional (NEQC), Departamento de Química (ICE), Universidade Federal de Juiz de Fora, 36.036-900 Juiz de Fora MG, Brazil, Steacie Institute for Molecular Sciences, NRC, Ottawa K1A 0R6, Canada, and Grupo de Pesquisa em Química Inorgânica Teórica (GPQIT), Departamento de Química, ICEx, Universidade Federal de Minas Gerais, 31.270-901 Belo Horizonte MG, Brazil

Received: December 28, 2006; In Final Form: February 16, 2007

Structure and dynamics of β-cyclodextrin (β-CyD), a prototype host for inclusion compounds of biological interest, is investigated by means of density-functional based tight-binding molecular dynamics (MD) simulations. The computational protocol is benchmarked against available experimental data and first-principles calculations. Solvent−solute interactions, including the diffusion into and dwell time of the solvent in the cavity of β-CyD, are studied with a hybrid QM/MM method. Comparison of MD simulations of β-CyD in the gas phase and in water shows that the solvent reduces the flexibility of the structure framework, while the terminal hydroxyl groups become more flexible and are embedded in a network of hydrogen bonds. Our 160 ps MD simulations, provide enough sampling to discuss the dynamics of the water inside the cavity. The dwell time of the encapsulated water molecule has a wide distribution with a peak at 70 fs. Surprisingly, despite only the 17% difference between the "top" and "bottom" opening area of the β-CyD cone, 64% of the water molecules enter the cavity through the slightly bigger "bottom" aperture.

1. Introduction

Cyclodextrins (CyD) have been extensively studied in the past decades, both experimentally and theoretically.[1−8] They are starch-derived cyclic oligomers with the main representatives formed by 6 (for α-CyD), 7 (for β-CyD), or 8 (for γ-CyD) glucose units. All cyclodextrins have the shape of a truncated cone enclosing a hydrophobic cavity. The inner cavity makes cyclodextrins particularly useful as hosts for inclusion compounds. In β-CyD, the cavity has "top" and "bottom" orifice diameters of respectively 6.0 and 6.5 Å, and a depth of 7.9 Å (see Figure 1).[9] The cavity is large enough to host many biologically active molecules, which suggests a principal application of CyDs as a drug carrier.[10] Inclusion phenomena of cyclodextrins, mostly of β-CyD, have been subject of many studies (for a review see ref 7). A considerable amount of data has been accumulated on the stability of cyclodextrin complexes in solution and on their thermodynamic and structural properties.[1,4,8,11] Still, the inclusion mechanism, which is of utmost importance for applications of CyDs in self-assembling and nanoreactors systems,[2,12,13] is not yet fully understood. Most of the reactions involving β-CyD as inclusion host take place in aqueous environment. A hydrophobic guest molecule can only be encapsulated by CyD if the interior water molecules, attached by hydrogen bonds, are removed. Therefore, interaction between β-CyD with water is of fundamental importance. X-ray[14] and neutron diffraction[15,16] studies show that, on average, about seven water molecules are located inside the cavity. At low temperatures (120 K) all 7 water positions are fully occupied.[16] In contrast, quasielastic neutron scattering[17] at room-temperature revealed an extensive positional disorder of water molecules inside β-CyD, with only 3 water positions fully occupied.

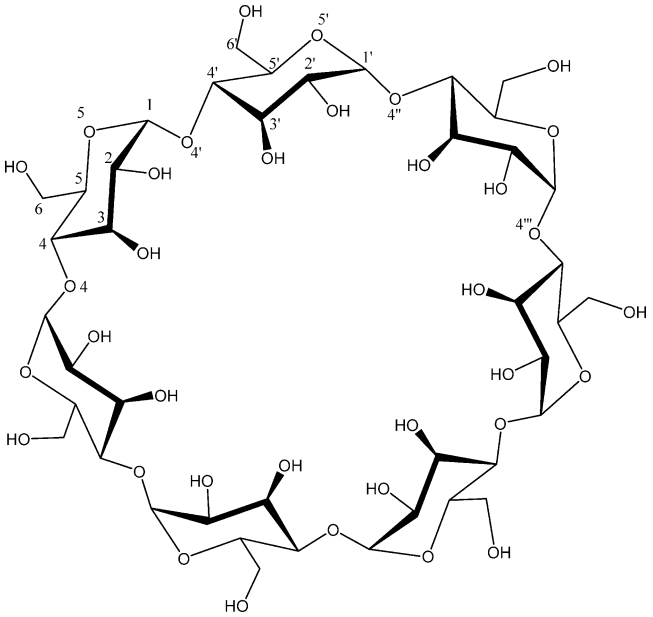

Figure 1. Structure of the β-CyD including the numbering scheme used to define the structural parameters. Dihedral angles: Φ, [C2C1O4′C4′], Ψ, [C1O4′C4′C3′], Ω, [O5C5C6O6], Γ, [C1C2C3C4], T, [C3C4C5O5], K, [O2C2C1O5], Y, [O3C3C4C5], Θ, [C2C3C4C5], Π, [C4C5O5C1], Ξ, [C4C5C6O6], ϑ, [O4C4C5O5], Z, [O4C4C5C6], Λ, [O4′C1O5C5], E, [C1O4′C4C5], τ, [O4O4′O4″O4‴]. Angles: θ, [C1O4′C4′], α, [O4O4′O4″], β, [OOH]. See text for detail.

† Part of the "DFTB Special Section".

* Corresponding author. E-mail: duarteh@ufmg.br. Phone: +55-31-3499-5748. Fax: +55-31-3499-5700.

‡ TU Dresden.

§ Universidade Federal de Juiz de Fora.

Steacie Institute for Molecular Sciences.

⊥ Universidade Federal de Minas Gerais.

10.1021/jp068988s CCC: $37.00
Published on Web 04/03/2007

Sophisticated experimental techniques, such as ultrafast guest dynamics, are currently used to explore the nanocavities.[1,18] In this paper, we will try to assist these investigations with density-functional tight-binding (DFTB) Born−Oppenheimer molecular dynamics simulations of the structure and dynamics of β-CyD and encapsulated water in aqueous solution.

Computational chemistry techniques have been widely used to study cyclodextrins.[3] Most of these investigations are, however, restricted to semiempirical methods[19,20] or empirical force fields.[21−25] The structure and dynamics of β-CyD in water have been studied to understand its behavior in the condensed phase.[26−31] The β-CyD molecule contains 147 atoms. Its structure (See Figure 1) and, consequently, the size of its cavity depend strongly on the presence of solvent and on the temperature. To account for the finite-temperature effects, molecular dynamics simulations with explicit inclusion of solvent molecules are necessary. Up to now, quantum mechanical (QM) dynamical simulations of cyclodextrins were impossible, either because of the cost or due to a poor description of weak interactions by many approximate QM methods. As a compromise between a first-principle method and an empirical force field, we decided to employ a hybrid QM/MM technique,[32] which treats the solvent using molecular mechanics (MM) and β-CyD quantum mechanically. To allow simulations approaching the nanosecond time scale, while permitting extension to β-CyD with encapsulated guest molecules and to larger CyDs, we use density-functional based tight-binding (DFTB) approach with self-consistent charge (SCC)[33] and London dispersion (DC)[34,35] corrections for the QM part. This method provides reliable results for biological and organic molecules.[36,37] We have shown recently that it is reliable for the calculation of structure and energies of β-CyD inclusion compounds.[38]

This article compares the structure and dynamics of β-CyD in the gas phase and in aqueous solution. We establish a computational protocol that allows simulations of inclusion compounds with β-CyD on the nanosecond time scale. We show that the results are consistent with the available experimental data. For simpler model systems, our results are in close agreement with predictions from more sophisticated quantum-mechanical techniques. Further, we explore properties of the cavity of β-CyD, the structure of the encapsulated water and calculate the dwell time of water in the cavity.

2. Computational Aspects

All calculations have been performed with the experimental version of the deMon code, which is available free of charge for personal and academic use.[39] For benchmark calculations of gas-phase β-CyD, gradient-corrected density-functional theory employing PBE functional[40] and DZVP basis set[41] were used. For QM/MM calculations, the QM part has been treated with the DFTB method[42,43] including the second-order density correction scheme (self-consistent charge, SCC)[33] and the correction for London dispersion (dispersion correction, DC)[34,35] as implemented in deMon (DC-SCC-DFTB).[35] The SCC-DFTB method has been thoroughly tested for biological molecules by Elstner and co-workers.[44,45] Hybrid QM/MM calculations applying SCC-DFTB to systems of biological interest have been reported earlier.[34,46,47] The molecular mechanics part employs Rappé's universal force field (UFF),[48] with the solvent partial charges taken from the TIP3P interaction potential for water (q(O) = −0.834, q(H) = 0.417).[49]

The UFF forcefield specifies "QEq" charges[50] on all atoms. For the water molecule, the QEq procedure leads to the partial charge on hydrogen of +0.353e. These charges would be suitable to describe a free water molecule. Used with a nonpolarizable force field, they are inappropriate for simulations of condensed water phases.[49] On the other hand,TIP3P partial charges (q(H) = +0.417e) account for polarization effects in condensed water phases. Used with the rigid water model, these charges reproduce many properties of bulk water phases.[49] The performance of the UFF flexible water model together with slightly modified TIP3P partial charges (q(H) = +0.41e) for bulk water and mixed water−alcohol phases was investigated by Zhen et al.[51] As an additional check for the hybrid UFF/TIP3P water potential, we determined the self-diffusion coefficient of water at ambient conditions, which was not considered by ref 51. The calculated value of 3.37×10^{-5} cm^2/s is somewhat higher than that in experiment (2.30×10^{-5} cm^2/s[52]), in close agreement with other TIP3P-based force fields.[53]

We implemented a QM/MM[32] subtraction scheme with electrostatic embedding in the deMon code,[39] for use in simulations of polar solutions. The technique is identical to the DFTB/CHARMM implementation[34] and allows the electrostatic embedding of the QM part in a field of fixed charges. Our implementation allows finite clusters as well as periodic boundary conditions (used in this work). In the implementation of ref 34, an addition scheme was employed to calculate QM/MM energies and forces:

$$E = E_{\mathrm{QM}}(\mathrm{S}) + E_{\mathrm{MM}}(\mathrm{T-S}) + E_{\mathrm{QM-MM}}$$
$$\vec{F} = \vec{F}_{\mathrm{QM}}(\mathrm{S}) + \vec{F}_{\mathrm{MM}}(\mathrm{T-S}) + \vec{F}_{\mathrm{QM-MM}}$$
$$E_{\mathrm{QM-MM}} = \sum_{i\in\{\mathrm{QM}\}}\sum_{j\in\{\mathrm{MM}\}} \frac{q_i q_j}{R_{ij}} + U_{\mathrm{vdW}}(R_{ij}) \qquad (1)$$

where T describes the total system and S denotes the subsystem that is calculated quantum-mechanically. The QM index indicates quantities calculated quantum mechanically, MM those calculated using molecular mechanics, and QM−MM gives the interaction between the two regions, calculated using the MM equations, using Mulliken charges determined quantum mechanically. As no bonds are broken, the latter contains only contributions from the Coulomb and van-der-Waals interactions. The charges of the MM region are included in the Hamiltonian and polarize the electronic density of the embedded structure. In the standard formulation of DFTB, the electrostatic term describing the Coulomb interaction between QM and MM regions already appears in the total energy and has to be removed from $E_{\mathrm{QM-MM}}$[34] to avoid double-counting.

In contrast to ref 34, the deMon implementation employs a subtraction scheme:

$$E = E_{\mathrm{MM}}(\mathrm{T}) + E_{\mathrm{QM}}(\mathrm{S}) - E_{\mathrm{MM}}(\mathrm{S})$$
$$\vec{F} = \vec{F}_{\mathrm{MM}}(\mathrm{T}) + \vec{F}_{\mathrm{QM}}(\mathrm{S}) - \vec{F}_{\mathrm{MM}}(\mathrm{S}) \qquad (2)$$

To allow calculations employing mechanical and electrostatic embedding using eqs 2, we choose to remove the term accounting for the Coulomb interactions between the QM and the MM region from the QM total energy and its gradients, and include it in $E_{\mathrm{MM}}(T)$. The resulting equations are equivalent those of ref 34 but leave the general appearance of the mechanical embedding subtraction scheme untouched.

In this work, the QM region contains β-CyD as solute. The MM region contains all water molecules. Therefore, there are no covalent interactions between QM and MM regions. The solvent influences β-CyD electronically by polarization of the electron density and mechanically through the Coulomb interac-

tions between Mulliken charges of the QM region with the TIP3P charges of the MM water. Van-der-Waals interactions between solute and solvent, and between solvent molecules, are treated using the Lennard-Jones potential of UFF, with C_6 and C_{12} parameters kept constant during the simulation.

We employ periodic boundary conditions (PBC) in the simulation. The Γ-point approximation is used for the DFTB electronic structure calculation. The long-range Coulomb interactions are treated with the Ewald technique. Evaluation of the shorter-range van-der-Waals interactions is restricted to atom pairs satisfying the minimum image convention. In constant-volume simulations using a sufficiently large cell, this approximation leads to an inconsequential constant shift of the potential energies, and has no effect on the geometries. Minimum image convention also eliminates possible discontinuities in the potential and forces, which may arise in the presence of long-range interaction cut-offs. All simulations use a 34.9 Å cubic box, containing 1385 water molecules (0.973 g cm^{-3}) and a single β-CyD molecule (0.044 g cm^{-3}).

During the Born−Oppenheimer molecular dynamics simulations, all trajectories have been carefully heated up, followed by 20 ps equilibration run using Berendsen thermostat[54] with a coupling parameter of $\tau = 0.1, ..., 1$ ps. For the microcanonical NVE (constant number of particles, volume, and energy) production run of 0.16 ns, a time step of 0.5 fs was chosen. The total energy remained constant within 0.001 Hartree during the whole simulation, with no systematic drift. The average temperature during the production run was 303 ± 3 K.

Technical details for calculation of radial functions and diffusion coefficients are given in the respective sections.

3. Results and Discussion

Cyclodextrin in the Gas Phase. We optimized the gas-phase structure of β-CyD as a benchmark for the DC-SCC-DFTB method. The optimized parameters of the β-CyD gas-phase structure are compared with a GGA-DFT calculation and with experiment in Table 1. The reported values are the arithmetic average between the equivalent distances, angles, and dihedrals in β-CyD (see Figure 1). It is interesting to observe that the DC-SCC-DFTB optimized structure is in good agreement with experiment (X-ray of crystalline β-CyD),[14−16] as well as with GGA-DFT (PBE/DZVP) calculations and recently reported parameters obtained at the HF/6-31G(d) level.[55] The backbone of the β-CyD structure, represented by the Γ, T, Z, Π, Λ, Θ, and ϑ dihedrals (Figure 1), is well described by the DC-SCC-DFTB Hamiltonian with deviations below 8° from the experiment. The Φ and Ψ dihedral angles are related to the relative position between the different glucose monomers. The DC-SCC-DFTB optimized values for Φ and Ψ are 231° and 122°, respectively. Although Φ is in good agreement with experiment, DC-SCC-DFTB underestimates Ψ by about 6°, in contrast to Hartree−Fock and GGA-DFT calculations, as well as experiment. The dihedrals Ξ and Ω show large variations between different sites, independent of the employed theoretical and experimental methods. These values are defined with respect to the primary hydroxyls (O6), which can rotate nearly freely. No meaningful fixed value can be assigned to these parameters. The conformation of the secondary hydroxyl is described by the K and Y dihedral angles. Their calculated values are very close to the experimental data, indicating that these groups are almost rigid due to the intramolecular hydrogen bonds. The τ dihedral angle is related to the adjacent glycosidic oxygens. This is another important structural parameter as it provides information about the deformation of the cavity. Theory and experiment agree that it has a minimum at $\tau \approx 0°$. The bond angles of the glycosidic framework are defined by the adjacent oxygens (α) and by C1O4′C4′ (θ). All theoretical methods and experiment agree to within 5° for these quantities.

TABLE 1: Structural Parameters Calculated for β-CyD at the DC-SCC-DFTB and DFT/PBE Levels of Theory[a]

	DC-SCC-DFTB	PBE/DZVP	DC-SCC-DFTB/ MM MD	XRD[b]
		Dihedral Angles		
Γ	307.6 ± 0.9	304.8 ± 0.9	310 ± 7	306 ± 3
T	305 ± 1	305 ± 2	309 ± 8	304 ± 4
Θ	53 ± 1	54 ± 2	48 ± 7	55 ± 3
Π	60.8 ± 0.8	60 ± 2	59 ± 8	59 ± 3
Φ	231 ± 8	224 ± 14	228 ± 16	231 ± 6
Ψ	122 ± 11	129 ± 6	124 ± 18	128 ± 9
ϑ	187 ± 2	187 ± 3	207 ± 14	188 ± 4
Λ	57.9 ± 0.9	59 ± 2	81 ± 18	59 ± 2
E	284 ± 10	276 ± 5	250 ± 19	285 ± 3
Ω	189 ± 113	190 ± 114	203 ± 82	198 ± 123
Ξ	104 ± 80	106 ± 78	99 ± 43	112 ± 70
Z	68 ± 2	68 ± 3	41 ± 82	69 ± 5
K	179 ± 2	182 ± 1	171 ±39	178 ± 3
Y	173 ± 1	175 ± 2	169 ± 37	176 ± 2
τ	−0.2 ± 14	0 ± 5	4.6 ± 19	0.2 ± 9
		Angles		
θ	123 ± 17	116.9 ± 0.9	115 ± 3	118 ± 1
α	128 ± 3	129 ± 3	127 ± 9	128 ± 2
		Intramolecular Hydrogen Bonds		
r(O···O)	2.93 ± 0.03	2.93 ± 0.08	2.95 ± 0.14	2.850
r(H···O)	1.95 ± 0.03	2.04 ± 0.04	3.01 ± 0.37	
β	4 ± 1	11 ± 0.5	56 ± 43	

[a] The angles are given in degrees (deg). Hydrogen bond distances are in ångstrom (Å). Experimental X-ray diffraction (XRD) data are included for comparison. See Figure 1 for the definitions of structural parameters. [b] References 16 and 14.

Next, we analyzed the intramolecular hydrogen bonds. The secondary hydroxyls (O2 and O3) can form intramolecular hydrogen bridges which can be classified by following the O···O and O···H distances and the O−O−H angle (β). The O···O and O···H distances are about 2.93 and 1.95 Å, respectively, and the β angle is about 4°. These values are consistent with an intramolecular hydrogen bond, as it is expected from the O···O distance of the X-ray structure, which is approximately 2.85 Å. In conclusion, DC-SCC-DFTB describes the structure of β-CyD well, showing good agreement with higher level methods and with experiment.

We have also investigated the change of structure with temperature using gas-phase molecular dynamics simulations at the MM and DFTB levels. The mean values at ambient temperature have been compared with the optimized parameters, the latter ones referring to the classical structure at $T = 0$ K. At room temperature, β-CyD is completely distorted *in the gas phase* according to DFTB method, whereas the UFF forcefield predicts less distorted structures. The τ dihedral angle is 27 ± 16° and 14 ± 9° at the DFTB and MM levels, respectively. These values can be compared to the ideal value of 0° for a completely symmetric structure. The deviation from the mean value is evidence of flexibility of the β-CyD structure in the gas phase with respect to twisting of each glucose monomer around the axis formed by O4−O4′ atoms. The DFTB potential energy surface (PES) of β-CyD is flatter than the respective UFF MM PES. At the same time, the α angle, which is related to the distortion in the plane perpendicular to the principal axis along the cone, is about 124.5 ± 9° and 127.6 ± 5° at the DFTB and MM levels, respectively. These values are very close to the experimental and optimized angle of 128°. The standard deviation, given in Table 1, is now taken over all equivalent

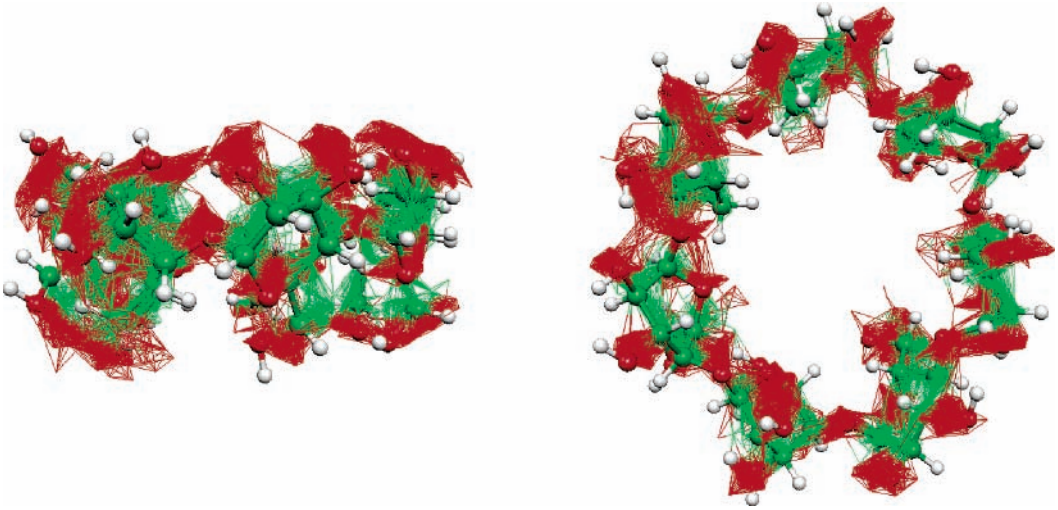

Figure 2. Configurational space taken by β-CyD in aqueous solution.

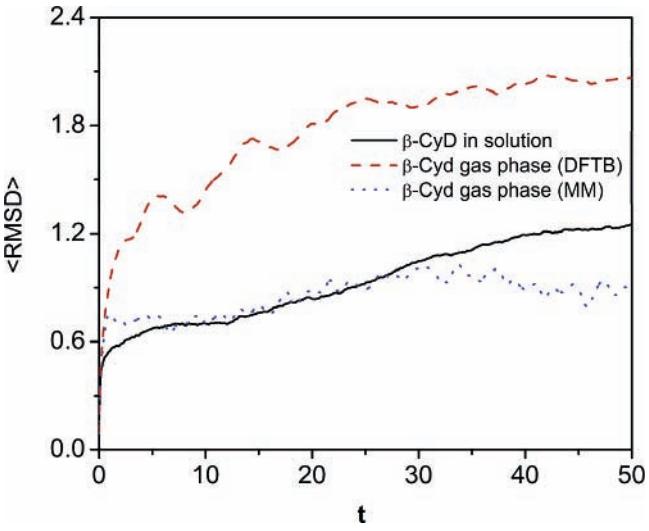

Figure 3. Root-mean-square deviation, <RMSD>, see eq 1, of the coordinates between a two snapshots of a MD trajectory (in Å) (gas phase in dashed red line) against simulation time t (in ps). The simulation in solution is given as black solid line, the DFTB and MM gas-phase simulation as dashed (red) line and dotted (blue) line, respectively.

sites and over several snapshots of the trajectory. The increase of the standard deviations, especially for the τ dihedral angle, indicates a large degree of fluxionality. The molecule recovers its ideal conformation when quenched to 0 K, as expected.

Cyclodextrin in Aqueous Solution. All computations reported in this section are performed using a hybrid QM/MM technique, as described above. The solvent-induced changes in the β-CyD structure are visualized in Figure 2, and can be quantified by the root-mean-square deviations (RMSD) of the coordinates between two snapshots of a MD trajectory, as proposed by Lawtrakul et al.[28] To account for long-time dynamical effects of the β-CyD, only heavy atoms are taken into account, and the time average over the trajectory is taken.

$$\langle \mathrm{RMSD} \rangle = \frac{1}{N_{\{C,O\}}} \sqrt{\sum_{k \in \{C,O\}} \langle |\vec{r}_k(t) - \vec{r}_k(0)|^2 \rangle} \qquad (3)$$

In eq 1, N denotes the number of non-hydrogen atoms of β-CyD.[18] Figure 3 shows $\langle$RMSD$\rangle$ plotted against simulation time for β-CyD in the gas phase and in solution. In solution, $\langle$RMSD$\rangle$ converges to an asymptotic value of approximately 1.2 Å. In the gas phase the molecule completely changes its geometry during the simulation at 300 K, converging to the value around 2.0 Å at the DFTB level of theory. Obviously, the water surrounding the β-CyD acts as a cushion, decreasing its free motion. Interestingly, this effect cannot be seen in pure MM calculations using the UFF force field. Obviously, the low-energy region of the PES for this force field is restricted to the area close to the experimental structure of the sugar, resulting in an excessively rigid sugar framework. As a result, UFF is not able to describe structures that change with temperature or environment, such as β-CyD. This highlights the potential of quantum-mechanical methods to describe molecules of biological interest, even if no chemical reaction takes place, as QM methods tend to show a much better transferability than a simple universal forcefield like UFF. A similar increase in flexibility could be expected from a more sophisticated classical forcefield.

In Table 1, structural parameters of the optimized β-CyD (theory) and crystal (experiment) are compared with those of β-CyD in aqueous solution. The latter ones are the time averages of the mean values, as discussed above. The mean values for the backbone structure of the cyclodextrin are not affected by the dynamics, and do not differ strongly from those of gas-phase simulation and crystal structure. For the glucose backbone, represented by the Π, Γ, Θ, and T dihedral angles, the differences are smaller than 6°. However, the standard deviation of these values increases by 8° in aqueous solution at ambient conditions. The dihedral angles involving the glycosidic oxygens (O4) (Ψ, Φ, ϑ, E, Λ) present much larger differences. The dihedrals related to the relative positions of the glucose monomers (Ψ, Φ) are in good agreement. The other dihedral angles (ϑ, E, Λ) are related to the twisting of one glucose monomer with respect to the remaining units along the principal axis of the cone. The difference is much larger, about 35°, with an even higher standard deviation (~20°) and shows that the cyclodextrin distortions are due to the high flexibility of the C1−O4−C4 bondings. This flexibility allows the β-CyD to distort in the plane perpendicular to the principal axis along the cone. The angles Ξ and Ω, which already indicate an appreciable mobility of the primary OH groups in gas phase, are now even more flexible and follow the direction of intermolecular hydrogen bridges with nearby waters. Torsions K and Y, which are related to the orientation of secondary hydroxyls, present high standard deviation and large differences compared to the gas-phase results, as expected. The intramolecular O···O distances increase slightly to 2.95 Å, compared

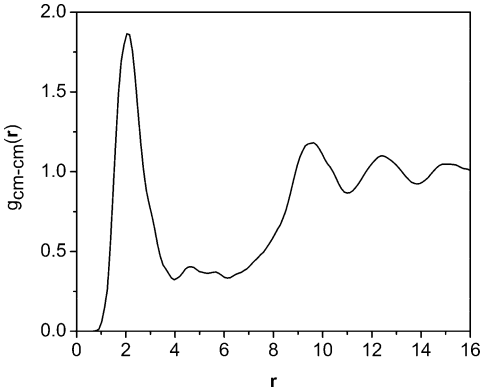

Figure 4. Radial distribution function for the distance (in Ångstrom) between the centers of mass of β-CyD and water molecules.

to 2.93 Å in gas phase. The O···H bridges observed in gas phase are broken at aqueous solution because the O···H average distance is increased to 3.01 Å. Hence, the internal hydrogen bonds are opened, and intermolecular bridges are favored instead. A further indication of the flexibility of the primary OH groups is the β angle (O−O−H), which is calculated to be $56 \pm 43°$. These findings demonstrate that β-CyD is extensively solvated in the water box. Another indication of structure deformation in solution is the τ dihedral angle, associated to the O4 glycosidic oxygens. It increases from 0° (gas phase) to 5°, which is associated with a distortion of β-CyD along principal axis of the cone, with a standard deviation about 9°.

Figure 4 shows the radial distribution function (RDF) of the centers of mass of water with respect to the center of mass of β-CyD. We find minima at 4.0, 10.9, and 13.8 Å. The first minimum corresponds to the encapsulated water molecules. The two outer minima arise from the first and second solvation shells of β-CyD, respectively. The position of first minimum in the RDF at around 4.0 Å corresponds roughly to the half of the depth of the β-CyD cavity. Integration over the RDF gives a value of 7.0, which means that, on average, 7 water molecules are inside the cavity. This result is in agreement with X-ray,[14] neutron diffraction,[15,16] and empirical force field[28] studies, which all arrived at 7 water molecules. The rim of β-CyD cavity corresponds to the range 4.0 and 7.3 Å in the RDF, and the outside region lies beyond 7.3 Å. The features of the RDF between 4.0 and 7.3 Å are related to water molecules that are weakly bonded to the primary and secondary OH groups at the rim of the cavity. The 7.0 water molecules inside of the cavity are interacting mostly with the glycosidic oxygens. Figure 5 illustrates the motion of the water molecules inside of the cavity and of the β-CyD structure during the dynamics.

As the final structural property, we analyze the formation of hydrogen bonds (HBs) between β-CyD and water. As suggested by Lawtrakul et al.,[28] we define the criterion for the existence of a hydrogen bond between donor (**D**) and acceptor (**A**) that (i) the D−A distance is less than the value corresponding to the first minimum of the respective O−O RDF, and (ii) the **D**H−**A** distance is less than 2.6 Å. The O−O RDF's, averaged over equivalent sites of β-CyD, are given in Figure 6 and show different maxima associated to the oxygens of the primary and secondary hydroxyls, and to the glycosidic and pyranoid oxygens. For the primary and secondary hydroxyls, we have the first minimum at about 4.4 Å, which integrate to 7.7 and 6.8 water molecules, respectively. For the glycosidic oxygens, a minimum is found at 3.85 Å, integrating to 1.1 water molecules. This minimum is mostly related to the encapsulated water molecules, and the small number of water molecules reflects the hydrophobicity of the cavity. For the pyranoid oxygens, a minimum representing 2.4 water molecules is observed at 4.0 Å.

Table 2 shows the average number of water molecules forming hydrogen bonds with the proton acceptor sites of β-CyD. In the following, we concentrate on the encapsulated water molecules. First, we determined the number of encapsulated ("Inner") waters forming hydrogen bonds. We find what 83% and 27% of the HBs of the glycosidic (O4) and pyranoid (O5) oxygens, respectively, are formed with the encapsulated waters. More than 92% of the HBs of the primary and secondary hydroxyls are formed with water molecules of the outer solvent. On average, 36% of the seven encapsulated waters form HBs with the glycosidic oxygens, and 25% with the pyranoid oxygens. It is important to note that the 8% of HBs of the primary and secondary hydroxyls are formed with the encapsulated water molecules. This is only possible because the solvated β-CyD at ambient conditions is extremely flexible, allowing the pyranoid rings to undergo major distortions needed to form these hydrogen bonds. The total number of HBs formed with β-CyD, including encapsulated waters and solvent, is on average 30.2, with 3.85 HBs that are due to the water molecules inside the cavity. This is in qualitative agreement with the

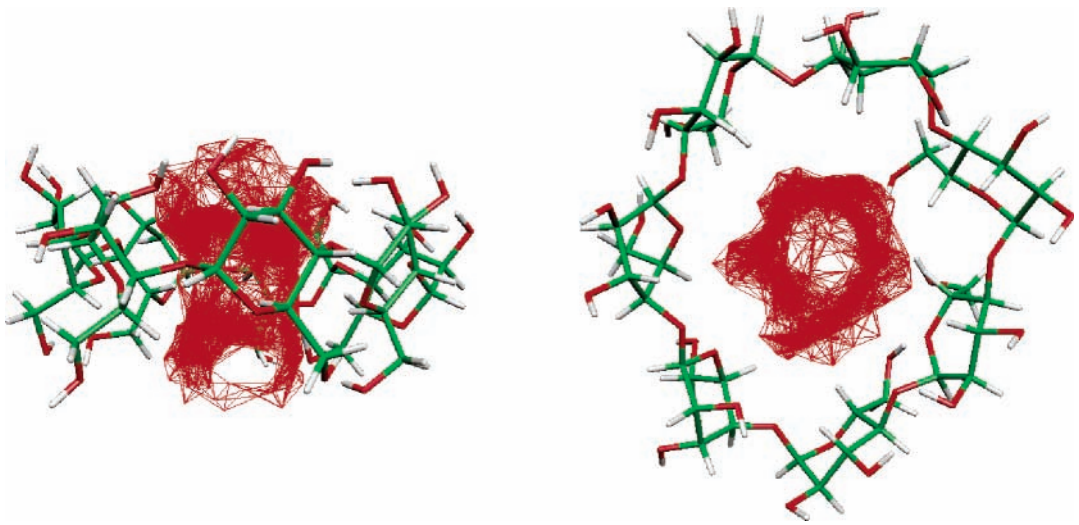

Figure 5. Configurational space taken by the water molecules encapsulated in β-CyD. For the sake of clarity, only the initial structure of β-CyD is shown.

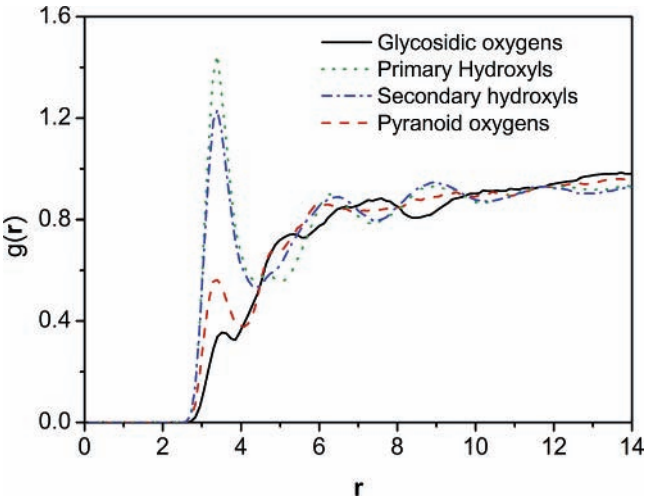

Figure 6. Radial distribution function $g(\mathbf{r})$ for H-bond sites in β-CyD and the centers of mass of the water molecules. Full line (black) represents the glycosidic hydroxyls; the dotted line (green), the primary hydroxyls; the dash dot line (blue), the secondary hydroxyls; and the dash line (red), the pyranoid oxygens.

TABLE 2: Average Number of Hydrogen Bonds and Corresponding Oxygen−Oxygen Distances between Water and β-CyD

binding site[a]	sites	av no.[b] total	av no.[b] inner	R(O···O) (Å)
O2/O3[c]	14	1.11 ± 0.89	0.05 ± 0.20	3.18 ± 0.17
O4	7	0.24 ± 0.46	0.20 ± 0.43	3.25 ± 0.17
O5	7	0.52 ± 0.64	0.14 ± 0.36	3.18 ± 0.19
O6	7	1.33 ± 0.96	0.11 ± 0.33	3.19 ± 0.16
Total		30.17 ± 26.88	3.85 ± 10.64	

[a] See Figure 1 for definition of atomic labels. [b] HBs averaged over equivalent atoms. "Inner" means that only water molecules inside of the cavity were considered. Standard deviations in the number of hydrogen bonds are also given. [c] Sites O2 and O3 are equivalent.

findings of Steiner et al.,[17] based on a quasielastic neutron scattering study of β-CyD, who showed that at room temperature the inner water molecules undergo an extensive positional disorder with only 3 water positions fully occupied.

It is interesting to note that similar analysis has been performed for the α-CyD using AMBER force field and Monte Carlo methods by Georg et al.[27] They found, on average, 5 water molecules inside the cavity, of which only 2.4 are hydrogen bonded to the α-CyD. Taking into account the relative size of the α- and β-CD, these results are in good relative agreement.

Next, we study the average dwell time of the water molecules in the cavity. Further, we examine through which opening the water enters and leaves the cavity. As mentioned above, β-CyD is a truncated cone with the "top" and "bottom" diameters being 6.0 and 6.5 Å. These values correspond to apertures of 36.0 and 42.3 Å^2, respectively. At a first glance, we would expect ≈17% more water molecules to enter or leave through the 17% larger bottom opening. We analyzed the water mobility profile by calculating the distribution of the dwell period along the trajectories (see Figure 7). There is a strong peak at 70 fs. However, we observe a very wide distribution of the dwell times, indicating that many water molecules remain in the cavity much longer, up to the entire length of simulation (160 ps).

We find that roughly two-thirds (64%) of the water molecules entered the cavity through the 17% larger bottom opening. This effect may arise due to synergy of two factors. Approximately one-third of the hydrogen bonds in solvated β-CyD is formed by the primary hydroxyl groups at O6. These hydrogen bonds

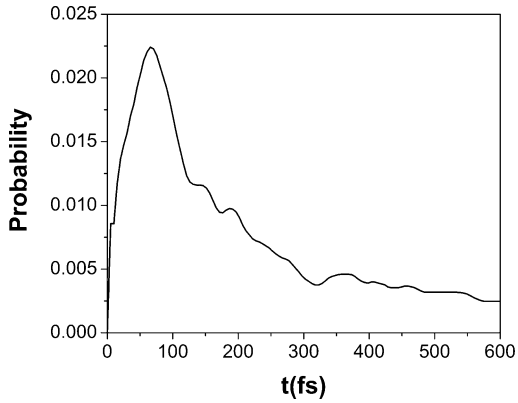

Figure 7. Residence time distribution of the water molecules inside the β-CyD inner cavity.

are involved in a robust interlocked network, reducing water mobility at the "top" aperture. At the same time, the flexible sugar backbone allows the "bottom" orifice to distort, accommodating solvent dynamics and increasing water mobility in this area. It seems that the combination of the two factors leads to a much more pronounced difference in water dynamics than one might expect from the purely geometrical difference of the bottom and top apertures.

4. Final Remarks

β-CyD in solution has been investigated at a hybrid quantum mechanics−molecular mechanics level. The solute was calculated using the quantum-mechanical DC-SCC-DFTB method, including a correction for dispersion. The surrounding water molecules were treated by the Rappé's universal force field. The simulation, at the nanosecond time scale, produces results that are within the error bars of available experiments. The free β-CyD molecule exhibits very large finite-temperature distortions from the ideal gas-phase geometry. However, in solution water molecules act as a cushion, restricting the motion of the β-CyD to the vicinity of the $T = 0$ K structure. Distortions of the C1−O4−C4 bond angles are responsible for the high flexibility of this molecule. The distortions in the plane perpendicular to the principal axis and twisting around the O4−O4′ axes of each monomer are due primarily to the flexibility of the C1−O4−C4 fragments. The backbone of the glucose monomer remains relatively rigid. Hydrogen bonding analysis shows that 36% of the encapsulated water molecules are forming HBs with the glycoside oxygens and 25% with pyranoid oxygens. The dwell time of the encapsulated water molecules peaks at 70 fs but is highly non-Gaussian and can reach the nanosecond time scale. A strong preference was observed for water molecules entering the inner cavity through the slightly wider "bottom" aperture. About 64% of the water molecules enter the cavity through this opening, which presents a section area only 17% larger than the top side. This surprising dynamical feature is important for the understanding of the encapsulation process involving cyclodextrins. The mechanism of inclusion in the cyclodextrins should not be proposed solely on the basis of structural parameters but should consider the complex dynamics of the host molecule and the solvent.

Finally, the DC-SCC-DFTB/MM hybrid method for simulating β-CyD in solution is shown to be reliable and adequate for studies of inclusion processes in solution. Investigation of inclusion compounds using this approach is in progress.

Acknowledgment. Financial support of the bilateral PROBRAL action (CAPES-DAAD, Brazil-Germany) is gratefully

acknowledged. This work was partially supported by the Brazilian research agencies: Conselho Nacional para o Desenvolvimento Científico e Tecnológico (CNPq), Fundação de Amparo à Pesquisa do Estado de Minas Gerais (FAPEMIG), and PRONEX-FAPEMIG (EDT 2403/03).

References and Notes

(1) Douhal, A. *Chem. Rev.* **2004**, *104*, 1955.
(2) Engeldinger, E.; Armspach, D.; Matt, D. *Chem. Rev.* **2003**, *103*, 4147.
(3) Lipkowitz, K. B. *Chem. Rev.* **1998**, *98*, 1829.
(4) Schneider, H. J.; Hacket, F.; Rudiger, V.; Ikeda, H. *Chem. Rev.* **1998**, *98*, 1755.
(5) Szejtli, J. *Chem. Rev.* **1998**, *98*, 1743.
(6) Hedges, A. R. *Chem. Rev.* **1998**, *98*, 2035.
(7) Rekharsky, M. V.; Inoue, Y. *Chem. Rev.* **1998**, *98*, 1875.
(8) Connors, K. A. *Chem. Rev.* **1997**, *97*, 1325.
(9) Li, S.; Purdy, W. C. *Chem. Rev.* **1992**, *92*, 1457.
(10) Uekama, K.; Hirayama, F.; Irie, T. *Chem. Rev.* **1998**, *98*, 2045.
(11) Liu, L.; Guo, Q. X. *Chem. Rev.* **2001**, *101*, 673.
(12) Vriezema, D. M.; Aragones, M. C.; Elemans, J.; Cornelissen, J.; Rowan, A. E.; Nolte, R. J. M. *Chem. Rev.* **2005**, *105*, 1445.
(13) Conn, M. M.; Rebek, J. *Chem. Rev.* **1997**, *97*, 1647.
(14) Lindner, K.; Saenger, W. *Carbohydr. Res.* **1982**, *99*, 103.
(15) Steiner, T.; Koellner, G. *J. Am. Chem. Soc.* **1994**, *116*, 5122.
(16) Zabel, V.; Saenger, W.; Mason, S. A. *J. Am. Chem. Soc.* **1986**, *108*, 3664.
(17) Steiner, T.; Saenger, W.; Lechner, R. E. *Mol. Phys.* **1991**, *72*, 1211.
(18) Barr, L.; Dumanski, P. G.; Easton, C. J.; Harper, J. B.; Lee, K.; Lincoln, S. F.; Meyer, A. G.; Simpson, J. S. *J. Inclusion Phenom. Macrocyclic Chem.* **2004**, *50*, 19.
(19) Dos Santos, H. F.; Duarte, H. A.; Sinisterra, R. D.; Mattos, S. V. D.; De Oliveira, L. F. C.; De Almeida, W. B. *Chem. Phys. Lett.* **2000**, *319*, 569.
(20) Nascimento, C. S.; Dos Santos, H. F.; De Almeida, W. B. *Chem. Phys. Lett.* **2004**, *397*, 422.
(21) Bea, I.; Gotsev, M. G.; Ivanov, P. M.; Jaime, C.; Kollman, P. A. *J. Org. Chem.* **2006**, *71*, 2056.
(22) Burusco, K. K.; Ivanov, P. M.; Jaime, C. *Arkivoc* **2005**, 287.
(23) Ivanov, P. M.; Jaime, C. *J. Phys. Chem. B* **2004**, *108*, 6261.
(24) Ivanov, P. M.; Jaime, C. *J. Mol. Struct.* **1996**, *377*, 137.
(25) Ivanov, P. M.; Jaime, C. *Ann. Quim.* **1996**, *92*, 13.
(26) Klepko, V.; Ryabov, S.; Kercha, Y.; Bulavin, L.; Bila, R.; Slisenko, V.; Vasilkevich, O.; Krotenko, V. *J. Mol. Liq.* **2005**, *120*, 67.
(27) Georg, H. C.; Coutinho, K.; Canuto, S. *Chem. Phys. Lett.* **2005**, *413*, 16.
(28) Lawtrakul, L.; Viernstein, H.; Wolschann, P. *Int. J. Pharm.* **2003**, *256*, 33.
(29) Winkler, R. G.; Fioravanti, S.; Ciccotti, G.; Margheritis, C.; Villa, M. *J. Comput.-Aided Mol. Des.* **2000**, *14*, 659.
(30) Koehler, J. E. H.; Saenger, W.; Vangunsteren, W. F. *J. Biomol. Struct. Dyn.* **1988**, *6*, 181.
(31) Koehler, J. E. H.; Saenger, W.; Vangunsteren, W. F. *Eur. Biophys. J. Biophys. Lett.* **1987**, *15*, 211.
(32) Warshel, A.; Levitt, M. *J. Mol. Biol.* **1976**, *103*, 227.
(33) Elstner, M.; Porezag, D.; Jungnickel, G.; Elsner, J.; Haugk, M.; Frauenheim, T.; Suhai, S.; Seifert, G. *Phys. Rev. B: Condens. Matter Mater. Phys.* **1998**, *58*, 7260.
(34) Cui, Q.; Elstner, M.; Kaxiras, E.; Frauenheim, T.; Karplus, M. *J. Phys. Chem. B* **2001**, *105*, 569.
(35) Zhechkov, L.; Heine, T.; Patchkovskii, S.; Seifert, G.; Duarte, H. A. *J. Chem. Theory Comput.* **2005**, *1*, 841.
(36) Elstner, M.; Frauenheim, T.; Kaxiras, E.; Seifert, G.; Suhai, S. *Phys. Stat. Solidi B-Basic Res.* **2000**, *217*, 357.
(37) Frauenheim, T.; Seifert, G.; Elstner, M.; Hajnal, Z.; Jungnickel, G.; Porezag, D.; Suhai, S.; Scholz, R. *Phys. Stat. Solidi B-Basic Res.* **2000**, *217*, 41.
(38) Lula, I.; Gomes, M. F.; Piló-Veloso, D.; De Noronha, A. L. O.; Duarte, H. A.; Santos, R. A. S., Sinisterra, R. D. *J. Inclusion Phenom. Macrocyclic Chem.* **2006**, *56*, 293.
(39) Köster, A. M.; Flores, R.; Geudtner, G.; Goursot, A.; Heine, T.; Patchkovskii, S.; Reveles, J. U.; Vela, A.; Salahub, D. R. deMon; NRC: Canada, 2004.
(40) Perdew, J. P.; Burke, K.; Ernzerhof, M. *Phys. Rev. Lett.* **1996**, *77*, 3865.
(41) Godbout, N.; Salahub, D. R.; Andzelm, J.; Wimmer, E. *Can. J. Chem.-Rev. Can. Chim.* **1992**, *70*, 560.
(42) Porezag, D.; Frauenheim, T.; Kohler, T.; Seifert, G.; Kaschner, R. *Phys. Rev. B: Condens. Matter Mater. Phys.* **1995**, *51*, 12947.
(43) Seifert, G.; Porezag, D.; Frauenheim, T. *Int. J. Quantum Chem.* **1996**, *58*, 185.
(44) Zhou, H. Y.; Tajkhorshid, E.; Frauenheim, T.; Suhai, S.; Elstner, M. *Chem. Phys.* **2002**, *277*, 91.
(45) Bohr, H. G.; Jalkanen, K. J.; Elstner, M.; Frimand, K.; Suhai, S. *Chem. Phys.* **1999**, *246*, 13.
(46) Elstner, M.; Frauenheim, T.; Suhai, S. *J. Mol. Struct.* **2003**, *632*, 29.
(47) Han, W. G.; Elstner, M.; Jalkanen, K. J.; Frauenheim, T.; Suhai, S. *Int. J. Quantum Chem.* **2000**, *78*, 459.
(48) Rappe, A. K.; Casewit, C. J.; Colwell, K. S.; Goddard, W. A.; Skiff, W. M. *J. Am. Chem. Soc.* **1992**, *114*, 10024.
(49) Jorgensen, W. L.; Chandrasekhar, J.; Madura, J. D.; Impey, R. W.; Klein, M. L. *J. Chem. Phys.* **1983**, *79*, 926.
(50) Rappe, A. K.; Goddard, W. A. *J. Phys. Chem.* **1991**, *95*, 3358.
(51) Zheng, J.; Balasundaram, R.; Gehrke, S. H.; Heffelfinger, G. S.; Goddard, W. A.; Jiang, S. Y. *J. Chem. Phys.* **2003**, *118*, 5347.
(52) Mills, R. *J. Phys. Chem.* **1973**, *77*, 685.
(53) Price, D. J.; Brooks, C. L. *J. Chem. Phys.* **2004**, *121*, 10096.
(54) Berendsen, H. J. C.; Postma, J. P. M.; Vangunsteren, W. F.; Dinola, A.; Haak, J. R. *J. Chem. Phys.* **1984**, *81*, 3684.
(55) Britto, M.; Nascimento, C. S.; dos Santos, H. F. *Quim. Nova* **2004**, *27*, 882.